**Atmospheric
Chemistry
and Physics**
Discussions

Open Access

Seasonal trends in concentrations and fluxes of volatile organic compounds above central London
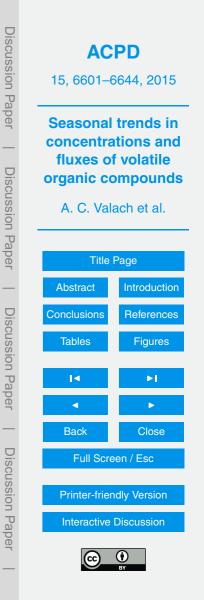
A. C. Valach[1,2], B. Langford[2], E. Nemitz[2], A. R. MacKenzie[3], and C. N. Hewitt[1]

[1]Lancaster Environment Centre, Lancaster University, Lancaster, LA1 4YQ, UK
[2]Centre for Ecology & Hydrology, Bush Estate, Penicuik, Midlothian, EH26 0QB, UK
[3]School of Geography, Earth and Environmental Sciences, University of Birmingham, Edgbaston, Birmingham, B15 2TT, UK

Correspondence to: C. N. Hewitt (n.hewitt@lancaster.ac.uk)

ACPD

15, 6601–6644, 2015

Seasonal trends in concentrations and fluxes of volatile organic compounds

A. C. Valach et al.

Title Page

Abstract	Introduction
Conclusions	References
Tables	Figures

|◄ | ►|
◄ | ►

Back | Close

Full Screen / Esc

Printer-friendly Version

Interactive Discussion

A. C. Valach et al.

Title Page

Abstract | Introduction

Conclusions | References

Tables | Figures

|◄ | ►|

◄ | ►

Back | Close

Full Screen / Esc
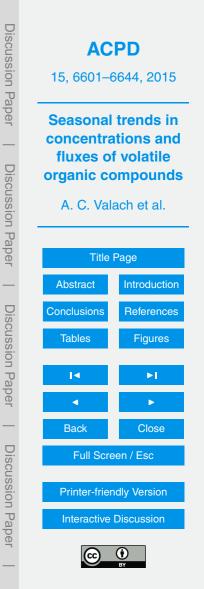
Printer-friendly Version

Interactive Discussion

Abstract

Concentrations and fluxes of seven volatile organic compounds (VOCs) were measured between August and December 2012 at a roof-top site in central London as part of the ClearfLo project (Clean Air for London). VOC concentrations were quantified using a proton transfer reaction-mass spectrometer and fluxes were calculated using a virtual disjunct eddy covariance technique. The median VOC fluxes, including aromatics, oxygenated compounds and isoprene, ranged from 0.07 to 0.33 mg m^{-2} h^{-1} and mixing ratios were 7.27 ppb for methanol (m/z 33) and <1 ppb for the remaining compounds. Strong relationships were observed between most VOC fluxes and concentrations with traffic density, but also with photosynthetically active radiation (PAR) and temperature for the oxygenated compounds and isoprene. An estimated 50–90 % of aromatic fluxes were attributable to traffic activity, which showed little seasonal variation, suggesting boundary layer effects or possibly advected pollution may be the primary causes of increased concentrations of aromatics in winter. PAR and temperature-dependent processes accounted for the majority of isoprene, methanol and acetaldehyde fluxes and concentrations in August and September, when fluxes and concentrations were largest. Modelled biogenic isoprene fluxes using the G95 algorithm agreed well with measured fluxes in August and September, due to urban vegetation. Comparisons of estimated annual benzene emissions from the London and National Atmospheric Emissions Inventory agreed well with measured benzene fluxes. Flux footprint analysis indicated emission sources were localized and that boundary layer dynamics and source strengths were responsible for temporal and spatial VOC flux and concentration variability during the measurement period.

1 Introduction

Currently over 50 % of the global population live in urban areas and with increasing trends in urbanization and population migration to urban centres, air quality remains

a high priority. Although in the UK volatile organic compound (VOC) emissions are subject to control under the European Commission Directive 2008/50/EC and emission reducing technologies have been implemented, urban air pollution continues to be a concern. VOCs from both anthropogenic and 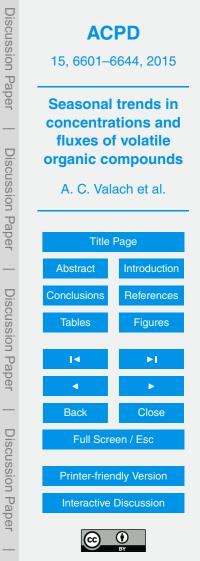biogenic sources impact urban air quality and climate through their contribution to tropospheric ozone and aerosol particle formation. Some VOCs are also carcinogens (e.g. benzene and 1,3-butadiene), which can directly affect human health (Kim et al., 2001). Most VOCs in urban areas are assumed to come from fuel combustion or evaporative emissions (Srivastava et al., 2005; Kansal, 2009). However, in summer, urban vegetation may additionally act as a source of VOCs such as methanol, isoprene and monoterpenes (Langford et al., 2009, 2010b).

Emission inventories such as the London and National Atmospheric Emissions Inventory use a "bottom-up" approach to estimate emission rates from pollutant sources which are temporally and spatially averaged. Micrometeorological eddy covariance techniques allow a "top-down" approach to quantify fluxes and these measurements can be compared with modelled emission estimates. Many compounds can have a variety of different sources which have yet to be identified and added to emissions inventories making "top-down" flux measurements vital. Satellite "top-down" approaches are available for only few chemicals (Lamsal et al., 2011), but not for primary VOCs. Biogenic isoprene can be indirectly quantified using satellite observations, but is subject to many uncertainties (Palmer et al., 2006). There have been few studies on VOC fluxes in urban areas which have been limited in spatial and temporal representation (Langford et al., 2009, 2010b; Velasco et al., 2005, 2009; Park et al., 2010, 2011). Due to the high technical demand of VOC flux measurements, it is difficult to increase spatial coverage. However, deploying instrumentation for long-term measurements provides better understanding of seasonal to annual variability.

In this study we present VOC flux and concentration measurements of seven selected compounds made over five months above central London using the virtual disjunct eddy covariance method. The aim of this study was to:

   i. Quantify VOC fluxes above an urban canopy using PTR-MS and eddy covariance;

   ii. investigate seasonal and spatial differences in VOC fluxes and

   iii. examine possible major source contributions of speciated VOCs.

These observations were made as part of the ClearfLo (Clean air for London) project which provided integrated short-term and long-term measurements of meteorology, gas phase and particulate pollutants over London and surrounding areas during 2011 and 2012 (Bohnenstengel et al., 2014).
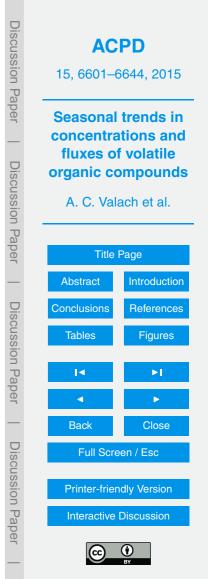
2 Methods

2.1 Measurement site

Micrometeorological flux measurements were made during the period from 7 August– 19 December 2012 from a flux tower located on the roof of a building belong- ing to King's College, University of London (51°30′42″ N 0°07′00″ W, ground altitude 30 m.s.l.) on the Strand in central London. Although the site is within the London Con- gestion Charge Zone (an area encompassing central London requiring road tolls to be paid regularly), surrounding roads supported a medium to high traffic volume (annual average of 50 000–80 000 vehicles per day, Department for Transport, 2014) with the river Thames situated 200 m to the south. This is an Oke (2006) urban class 2 site (intensely developed high density with 2–5 storey, attached or very close-set build- ings made of brick or stone, e.g. old city core). The inlet and sonic anemometer were mounted on a triangular mast (Aluma T45-H) at approx. 60.9 m (2.3× mean building height, z_H) a.g.l., several meters west of the KSS site (i.e. KSSW) used for long-term energy and CO_2 flux measurements (Kotthaus and Grimmond, 2012).The mean build- ing height was around 25 m and the mast was located on an elevated area in the centre of the roof. A street canyon was located directly to the NW and an enclosed parking area to the SE, but generally surrounding buildings were of equal height. Kotthaus and Grimmond (2013) describe in detail the measurement area and investigate the influ-

ence of source area characteristics on long-term radiation and turbulent heat fluxes for the KSS site, which is in the same area.
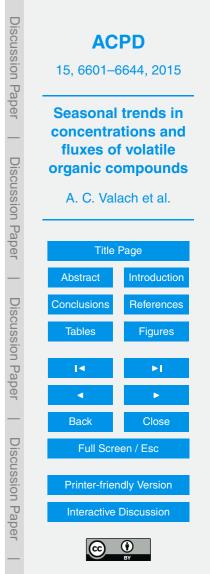
The weather in 2012 was somewhat cooler than the (1981 to 2010) long-term mean for London during summer and autumn, with several cold fronts bringing up to twice as much precipitation and associated winds suppressing pollution levels. During the Olympics and Paralympics (27 July–12 August and 29 August–9 September 2012) the weather was hot and dry causing sustained pollution peaks. Winter 2012/13 was generally warmer and drier in London than the 1981–2010 mean (Met Office, 2013).

2.2 Instrumentation and data acquisition

The CSAT3 sonic anemometer (Campbell Scientific) and inlet were facing toward the predominant wind direction (SW) to minimise flow distortion. Data from the sonic anemometer were logged at a frequency of 10 Hz and flux measurements were calculated using 25 min averaging periods. The rotation angle theta (θ), used to correct measurements of the vertical wind velocity for minor misalignment of the sonic anemometer, showed no significant disturbance of the turbulence from interactions with the building when plotted against wind direction. Data were recorded in UTC (Universal Time Coordinated) which is one hour earlier than local time in summer and coincident with Greenwich Mean Time in winter.
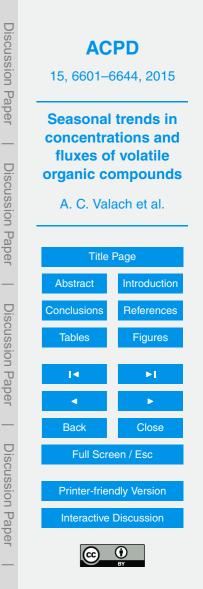
VOC concentrations were measured using a high sensitivity proton transfer reaction-(quadrupole) mass spectrometer (PTR-MS) (Ionicon Analytik GmbH, Innsbruck, Austria) with three Varian turbo-molecular pumps (see Lindinger et al., 1998; de Gouw and Warneke, 2007; Hayward et al., 2002 for more detailed description of the instrument). Air was drawn through an inlet co-located with the sonic anemometer on the flux tower approx. 60.9 m a.g.l. Sample air was purged through a $\sim$ 30 m 1/2$''$ OD (3/8$''$ ID) PTFE tube at a flow rate of 81 L min^{-1} to the PTR-MS, which was housed in a utility room below. The high flow rate ensured turbulent flow was maintained and signal attenuation minimised (Reynolds number, Re = 11 177). During the campaign, PTR-MS operating parameters were maintained at 1.95 mbar, 510 V and 50 °C for drift tube pressure, volt-

age and temperature respectively to achieve an E/N (E: electric field strength, N: buffer gas number density) ratio of 123 Td (1 Td = 10^{-17} V cm^2). This field strength forms a compromise between reagent ion clustering and fragmentation suppression (Hewitt et al., 2003). Further instrument parameters and meteorological conditions are summa-
5 rized in Table 1. The inlet flow rate into the instrument was held at 0.25–0.3 L min^{-1}. The logging program was written in LabVIEW (National Instruments, Austin, Texas, USA) and operated the PTR-MS in multiple ion detection (MID) and SCAN modes for VOC concentrations of nine selected masses and a range of the protonated mass spectrum m/z 21–206 respectively. A valve system controlled the measurement cycle consisting
10 of 5 min zero air (ZA), 25 min MID followed by further 5 min SCAN of sample air and 25 min MID mode. During the ZA cycle air was pumped through a custom-made gas calibration unit (GCU) fitted with a platinum catalyst heated to 200 °C to provide instrument background values at ambient humidity. In MID mode the quadrupole scanned nine predetermined protonated masses with a dwell time of 0.5 s each to which the
15 following compounds were ascribed: m/z 21 (indirectly quantified m/z 19 primary ion count [H$_3^{18}$O$^+$]), m/z 33 (methanol), m/z 39 (indirectly quantified m/z 37 first cluster [H$_3^{16}$O$^+$ H$_2^{16}$O$^+$]), m/z 42 (acetonitrile, results not shown), m/z 45 (acetaldehyde), m/z 59 (acetone/propanal), m/z 69 (isoprene/furan), m/z 79 (benzene), m/z 93 (toluene), m/z 107 (C$_2$-benzenes), and m/z 121 (C$_3$-benzenes, results not shown). The total
20 cycle time was 5.5 s. Secondary electron multiplier (SEM) voltage, as well as O$_2^+$ (m/z 32) and photon "dark counts" (m/z 25) signals were monitored weekly. The PTR-MS cannot distinguish between different compounds with the same integer mass, therefore isobaric interference can occur. For example, m/z 107 is considered to be the sum of several contributing C$_8$-aromatics: ethyl benzene, (m + p)-xylene, o-xylene and some
25 benzaldehyde (Warneke et al., 2003). Further interferences at measured m/z from additional compounds and fragmentation for this instrument in an urban environment are discussed in Valach et al. (2014). Although the O$_2^+$ and water cluster ions were kept < 2 % of the primary ion, interferences from ^{18}O$^+$ isotopes at m/z 33 were taken into account. The sonic anemometer was not directly interfaced with the LabVIEW log-

Title Page

Abstract | Introduction

Conclusions | References

Tables | Figures

|◀ | ▶|

◀ | ▶

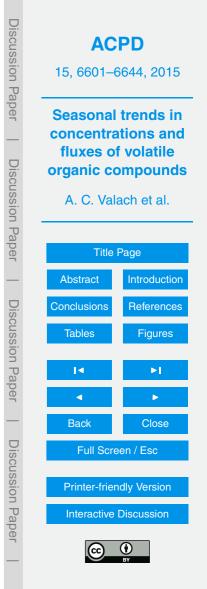Back | Close

Full Screen / Esc

ging program requiring the measurements to be synchronised during post-processing through the use of a cross-correlation function between the vertical wind velocity w and the VOC ion counts c.

Single point calibrations were performed on-site once a month using a certified multiple component VOC gas standard (Ionimed, since 23 May 2013 part of Ionicon Analytik GmbH, Austria), which was validated by cross-calibration with a second independent VOC standard (Apel Riemer Environmental Inc., CO, USA). Before and after the campaign multistep calibrations were performed with both standards. Standards were diluted with catalytically converted zero air, since cylinder concentrations were approx. 1 ppm ±5 % uncertainty (Ionimed Analytik) and 0.5 ppm ±10 % (Apel Riemer). Error propagation resulted in a total calibration uncertainty of < 20 %. Measured normalised instrument sensitivities (S_N, Table 1) based on Taipale et al. (2008) were used to convert normalised count rates (*ncps*) of protonated masses (RH$^+$) to volume mixing ratios (Langford et al., 2010a). Only the o-xylene isomer was present in the Ionimed standard, which was used to determine instrument sensitivities for m/z 107, but sensitivities agreed well when compared with sensitivities for p-xylene present in the Apel Riemer standard. Any remaining humidity effects on calibrations were previously investigated for this instrument and were found to be within the overall calibration uncertainty (Valach et al., 2014). Detection limits of VOC concentrations (Table 2) were calculated according to Taipale et al. (2008).

2.3 Flux calculations and quality assessment

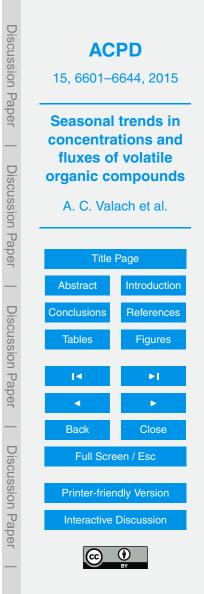Fluxes were calculated according to Karl et al. (2002) and Langford et al. (2009, 2010b) using:

$$F = \frac{1}{n} \sum_{i=1}^{n} w' \left(\frac{i - t_{lag}}{\Delta_{tw}} \right) \times c'(i) \tag{1}$$

where w' and c' are the instantaneous fluctuations around the mean vertical wind ($w - \overline{w}$) and mean VOC concentration ($c - \overline{c}$), n is the number of VOC concentration measurements per 25 min averaging period ($n = 273$), t_{lag} is the lag time between the wind and PTR-MS measurement due to the tr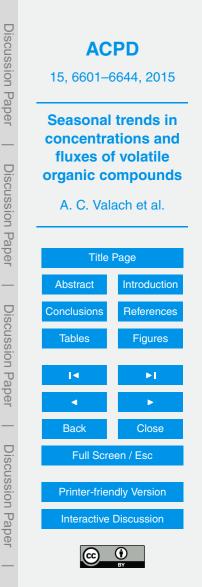ansit through the sampling line, and Δ_{tw} is the sampling interval of the vertical wind speed measurements of the sonic anemometer (10 Hz = 0.1 s). Langford et al. (2015) recently demonstrated that the method used to determine the time lag becomes important where the signal-to-noise ratio of the analyser is poor, showing that methods that systematically search for a maximum in the cross-correlation function within a given window (MAX method) can bias the calculated fluxes towards more extreme (positive or negative) values. Their study recommends the use of a prescribed lag time determined either through the use of a monitored sample flow rate or by using the typical lag time derived by searching for a maximum. Here the prescribed lag times were determined by fitting a running mean to the time series of daytime lag times calculated using the MAX method for acetone which had large fluxes and thus the clearest time-lags. Prescribed lag times for all other compounds were set relative to that of acetone, accounting for the offset introduced by the sequential sampling of the PTR-MS. Flux losses due to the attenuation of high and low frequency eddies were estimated for our measurement setup. High frequency flux attenuation was estimated to be on average 11 % using the method of Horst (1997), and a correction was applied. Attenuation from low frequency fluctuations for a 25 min flux period was investigated by re-analysing the sensible heat fluxes for longer averaging periods of 60, 90, 120 and 150 min. The coordinate rotation was applied to the joined files, which acted as a high pass filter to the three wind vectors, confirming that fluctuations of eddies with a longer time period than the averaging time did not contribute to the flux measurement (Moncrieff et al., 2004). The fluxes were compared back to the 25 min average fluxes, which had the coordinate rotation applied before joining, again to ensure only turbulent fluctuations of ≤ 25 min contributed to the flux (Fig. SA1). Flux losses due to low frequency attenuation were estimated to be < 1.5 % and, therefore, no corrections were deemed necessary.

Many of the 25 min resolved flux measurements were close to the limit of detection (LoD) based on 1 SD using the method of Spirig et al. (2005), with an average fail rate of 82 %. Various techniques to statistically analyse or replace values below the LoD have been developed (Clarke, 1998), however, they often result in significant bias, either high or low depending on the value substituted, because values tend to be below the LoD when fluxes are indeed small (Helsel and Hirsch, 1992). In this study, our analysis focused on diurnally averaged fluxes and we decided not to filter out individual flux values on the basis of being < LoD in order to avoid this bias. When averaging the 25 min flux data it is appropriate to also average the LoD which, as shown by Langford et al. (2015), decreases with the square root of the number of samples averaged (N). Therefore, although the majority of the individual 25 min flux measurements were below the LoD, their diurnal averages may exceed the LoD for the average and thus still yield important data on the net exchange of VOCs above the city.

$$\overline{\mathrm{LoD}} = \frac{1}{N}\sqrt{\sum_{i=1}^{N} \mathrm{LoD}^2} \tag{2}$$

The following describes the additionally applied filter criteria. 25 min flux values with a friction velocity (u_*) $< 0.15\,\mathrm{m\,s^{-1}}$ were rejected (3.4 % of total data) due to insufficient turbulence. The stationarity test and data quality rating methods of Foken and Wichura (1996) and Velasco et al. (2005) were used, and 47 % of the data files were rejected on this basis. The high number of files rejected in the stationarity test is to be expected for eddy covariance measurements over canopies where ergodicity cannot exist, although horizontally averaged canopy morphology recovers some planar homogeneity. Furthermore, the low measurement height can cause an increased sensitivity towards canopy roughness features resulting in non-stationarity. Since urban environments are not ideal for micrometeorological flux measurements, integral turbulence characteristics of this site were assessed by comparing the measured SD of the vertical wind velocity (σ_w) normalised by u_* to the parameters of a modelled ideal turbulence (Foken et al., 2004). Results showed that 99.6 % of all the data were rated

category six or better and 0.4 % were rejected using the criteria of Foken et al. (2004). This large pass rate gives further confidence that the measurements were not unduly affected by wake turbulence generated from the structure of the building. Erroneous meteorological data (2.6 % of total) were removed around wind directions of 14–15°,
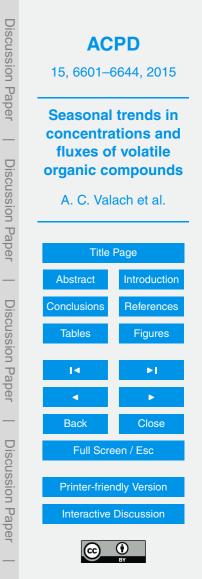
5 due to minor turbulence interferences from the presence of other sensors on the mast. Depending on compound between 40–61 % of flux data (N = 1934–2949) passed all of the above quality controls. 2014 h of concentration data (N = 4834) were obtained. For consistency regression coefficients (R^2) were used throughout.

The traffic densities used for the analysis were obtained from a nearby site at Maryle-

10 bone Road (approx. 3 km to the NW) and consisted of hourly vehicle counts covering the period 7 to 22 August 2012. The major roads of the Strand and the Embankment areas surrounding the measurement site support a comparable traffic volume with an annual average of 50 000–80 000 vehicles per day (Department for Transport, 2014) and diurnal patterns in traffic are likely to be similar across central London.

15 Photosynthetically active radiation (PAR) and CO_2 measurements used in the analysis were part of the KSS long-term micrometeorological measurements at the same site and covered the period from August to September for PAR and to December for CO_2 respectively.

2.3.1 Flux footprint calculations

20 Although there are no operational footprint models for urban environments which take the complex topography and spatial variability in building height and surface heat fluxes into account, the analytical footprint model suggested by Kormann and Meixner (2001) has previously been applied in non-homogeneous terrain (Helfter et al., 2011; Neftel et al., 2008). The Kormann–Meixner (KM) model determines the 2-D footprint den-

25 sity function explicitly from micrometeorological parameters, which are provided by the eddy covariance measurements, i.e., friction velocity (u_*), Obukhov length (L), horizontal wind velocity at the measurement height ($u(z_m)$), SD of the lateral wind (σ_v), and measurement height (z_m). The flux footprints were calculated for each 25 min flux

period. Neftel et al. (2008) developed a Microsoft Excel based tool, which allows the footprint contributions (%) of user-defined spatial elements to be mapped, in this case we used a total of nine $1\,km^2$ grid squares to match the Ordinance Survey (OS) grid (Fig. 1). This grid resolution was validated using a simple parameterisation model (Kljun et al., 2004) with diurnal average parameters for σ_w, u_*, and boundary layer height (z_i) during the campaign, which calculated the distance of the maximum flux contribution (X_{max}) and the extent of the 90% flux footprint (X_{90}).

The KM footprint calculation requires the Monin–Obukhov stability parameter (ζ) to be within the interval $[-3, 3]$, where
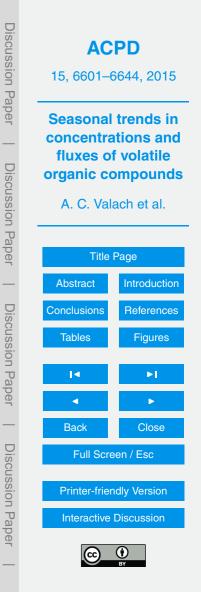
$$\zeta = \frac{z_m - d}{L}, \tag{3}$$

with d ($d = 2/3 z_H = 16.7\,m$) being the displacement height estimated as a fraction of the canopy height (Garrat, 1992). The footprint estimation for cases of extreme stability is of lower quality, but still provides useful information. The vertical turbulent flux F_c (0, 0, z_m) measured at the height z_m is related to the corresponding surface flux area F_c (x, y, 0) which is upwind of the measurement point, such that

$$F_c(0, 0, z_m - d) = \int_{\infty}^{-\infty} \int_0^{\infty} F_c(x, y, z_m - d) \Phi(x, y, z_m - d)\, dx\, dy \tag{4}$$

where z_m is the measurement height and the x axis is aligned with the mean horizontal wind direction. $\Phi(x, y, z_m - d)$ is the footprint function and includes a weighting function to describe the influence 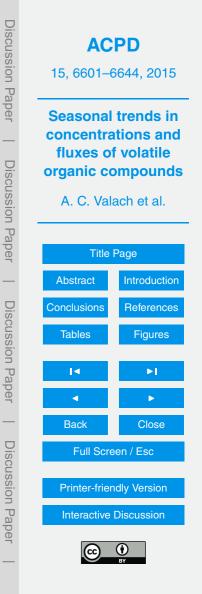of a unit point source on the flux from any surface location (x, y). In order to compare VOC fluxes with estimated emissions from the London Atmospheric Emissions Inventory (LAEI), the $1\,km^2$ OS grid system was used which on average included 90% of the footprint contribution to all measured fluxes. This area was limited to central London and partially included the following Boroughs: Westminster (squares 1, 4, 5 and 7), Southwark (2, 3 and 6), Camden (8) and the City of London (9) (Fig. 1).

3 Results and discussion

3.1 Diurnal profiles of VOC fluxes and concentrations

Diurnal averages of measured VOC fluxes and mixing ratios are shown in Fig. 2a and b with descriptive statistics for all the data summarized in Table 2. Toluene and C$_2$-benzenes showed the largest median fluxes (interquartile range in parenthesis) of 0.33 (0.04–0.91) mg m^{-2} h^{-1} and 0.30 (0.08–0.64) mg m^{-2} h^{-1} respectively, followed by oxygenated compounds, methanol (0.27 (0.12–0.42) mg m^{-2} h^{-1}), acetaldehyde (0.14 (0.06–0.23) mg m^{-2} h^{-1}), and acetone (0.22 (0.10–0.40) mg m^{-2} h^{-1}). Isoprene and benzene showed the smallest median fluxes with 0.09 (0.02–0.20) mg m^{-2} h^{-1} and 0.07 (0.002–0.18) mg m^{-2} h^{-1} respectively. The highest median mixing ratios were of the oxygenated compounds methanol (7.3 (6.8–7.9) ppb), acetone (0.95 ($<$ LoD–1.36) ppb) and acetaldehyde (0.82 (0.59–1.13) ppb), followed by aromatics (C$_2$-benzenes, toluene and benzene), and isoprene. Oxygenated compounds commonly have relatively long atmospheric lifetimes and widespread sources including anthropogenic, biogenic and some atmospheric sources, resulting in elevated concentrations and less pronounced diurnal profiles (Atkinson, 2000). Most VOC fluxes and concentrations were comparable to or lower than those previously observed in London (Langford et al., 2010b) and other UK cities (Langford et al., 2009), although C$_2$-benzene fluxes and concentrations, as well as isoprene and benzene concentrations were slightly higher. The discrepancy in isoprene and benzene concentrations is consistent with photochemical loss during transport to the higher measurement height of the previous study. Compared to Mexico City VOC fluxes were lower, apart from C$_2$-benzenes (Velasco et al., 2005).
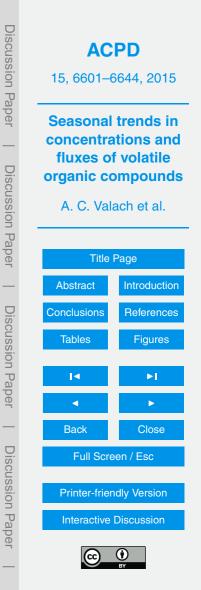
3.1.1 Correlations with possible controlling variables of VOC fluxes and concentrations

Aromatic compound fluxes followed the diurnal profile of traffic density with good correlations (R^2 = 0.51–0.92, $p < 0.05$) and slightly lower fluxes observed on the weekends. In central urban areas traffic densities – and therefore traffic-related VOC fluxes – increase steadily throughout the day, with discernible peaks during morning, midday and evening (Nemitz et al., 2002), which was also observed in this study. Diurnal profiles of concentrations for aromatics presented clear double rush-hour peaks during the morning and evening (07:00–10:00 and 17:00–20:00 LT), which is thought to be linked to advection from larger commuter roads outside of the city centre, as well as diurnal expansion and contraction of the boundary layer. This suggests that traffic-related emissions were the main contributors to fluxes and mixing ratios of aromatic compounds. Previous studies have shown that the Marylebone Rd traffic count point can be used as a proxy representative of traffic flows throughout central London (Helfter et al., 2011). The diurnal flux profiles of methanol, acetone, and isoprene, and to a smaller extent acetaldehyde, showed one large peak just after midday (approx. 13:00 local time). Vehicle emissions may have contributed to their levels directly or indirectly, since flux correlations of acetaldehyde and isoprene fluxes with traffic density were fairly high (R^2 = 0.60 and 0.46 respectively, $p < 0.05$). Their diurnal concentration profiles mimicked those of the fluxes with isoprene and acetaldehyde reflecting a slight double peak. Methanol has a relatively long atmospheric lifetime, hence mixing ratios showed no clear diurnal profile.
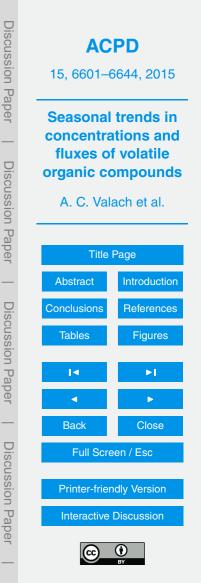
VOC fluxes and concentrations plotted as a function of photosynthetically active radiation (PAR) showed strong daytime (defined as 06:00 to 18:00 GMT) correlations for methanol, acetaldehyde and isoprene fluxes and concentrations (R^2 = 0.71–0.78 and 0.66–0.83, $p < 0.01$ respectively). Plotted as a function of temperature high correlations with methanol, acetaldehyde and isoprene fluxes (R^2 = 0.75, 0.63, and 0.94, $p < 0.001$ respectively) were seen, whereas only methanol and acetone concentrations

Full Screen / Esc

Printer-friendly Version

Interactive Discussion

showed higher correlations with temperature ($R^2 = 0.64$ and 0.81, $p < 0.001$ respectively). Methanol fluxes correlated linearly with temperature ($R^2 = 0.75$, $p < 0.001$), but acetaldehyde and isoprene had exponential relationships ($R^2 = 0.64$ and 0.94, $p < 0.01$) for fluxes and mixing ratios ($R^2 = 0.45$ and 0.55, $p < 0.01$) with temperature (Fig. 3 example of isoprene). The relationships of mixing ratios with PAR and temperature for these compounds improved greatly when excluding night time values (defined as PAR $< 100\,\mu mol\,m^{-2}\,s^{-1}$) and points of low temperature ($< 5\,^\circ C$), indicating either separate source contributions or effects of boundary layer meteorology in these instances. Increased mixing ratios of these compounds with low PAR and temperature are likely effects of reduced dilution within a shallow boundary layer, e.g., at night or in winter, but also possible contributions of anthropogenic sources such as exhaust emissions, which are largely independent of light and temperature. Increases in concentrations due to high PAR and temperature suggest biogenic sources, increased evaporative emissions, and/or secondary atmospheric formation driven by oxidation of precursor hydrocarbons (Singh et al., 1994). Oxygenated compounds have a variety of different source contributions such as tailpipe emissions, evaporative emissions from fuel and solvents, direct emissions from plants, leaf decomposition, and secondary atmospheric production (Langford et al., 2009 and references therein). Modelling studies have indicated that the contribution of secondary atmospheric formation to VOC concentrations could be more significant, especially in urban areas during summer, i.e. with high PAR and temperatures (Harley and Cass, 1994; de Gouw et al., 2005). De Gouw et al. reported that background values could be more important for methanol and acetone concentrations, which could cause changes in boundary layer meteorology to result in greater effects on observed concentrations. Furthermore, acetaldehyde concentrations are more often affected by secondary atmospheric formation. The observed light and temperature responses associated with isoprene fluxes and mixing ratios in August and September can be explained by biogenic sources (cf Sect. 3.1.3). Acetone fluxes reached a maximum when PAR and temperature were around $1000\,\mu mol\,m^{-2}\,s^{-1}$ and 15–20 $^\circ C$ respectively, before declining, whereas mixing ratios increased exponen-

Title Page

Abstract | Introduction

Conclusions | References

Tables | Figures

|◄ | ►|

◄ | ►

Back | Close

Full Screen / Esc

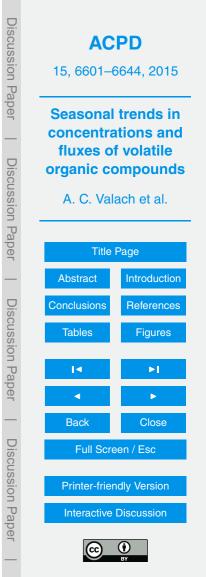Printer-friendly Version

Interactive Discussion

tially with light and temperature. These observations mimic measurements over forest canopies (Schade and Goldstein, 2001). Aromatic compound concentrations and fluxes showed no correlations with PAR. Weak negative correlations were seen with aromatic concentrations and temperature and weakly positive correlations with fluxes and temperature likely due to increased thermal mixing.

3.1.2 Seasonal variability of VOC sources and meteorology

Most compounds showed larger fluxes in August and September than in October, November and December, with the exception of acetaldehyde (Fig. 4a). Increased acetaldehyde fluxes in December may have resulted from an additional source, such as domestic biomass burning (Lipari et al., 1984; Andreae and Merlet, 2001), although there are only few residential buildings in this area of London. Only toluene fluxes in September were significantly higher than in other months and benzene fluxes showed no significant seasonal differences. Seasonal variability in fluxes was likely due to increased emissions in summer, especially for compounds with biogenic and secondary atmospheric sources. Average monthly meteorological parameters are summarized in Table 3.

Mixing ratios of aromatics were generally lower in summer and highest in December (Fig. 4b). This is likely due to less dilution effects in winter when the boundary layer is shallow or from advection of additional sources such as heating, since there was no increase in fluxes. Furthermore, traffic counts for the Congestion Charge Zone in central London indicate lower monthly average vehicle counts in December (DfT, 2014). Oxygenated compounds and isoprene mixing ratios were highest in summer with the exception of acetone, which increased in December likely either from boundary layer effects, reduced photochemical degradation, or advection. Mean daytime maxima of diurnal profiles for the boundary layer mixing height measured using three LiDARs located on rooftops within central London were between 1700 m in summer and 900 m in winter (Bohnenstengel et al., 2014). Increased summer mixing ratios of oxygenated compounds and isoprene indicated a temperature dependent, possibly biogenic source

Seasonal trends in concentrations and fluxes of volatile organic compounds

A. C. Valach et al.

contribution. While biogenic emissions may be advected from outside of the city, the concurrent increase in isoprene fluxes suggests the source to be largely local to the flux footprint. The temperature dependent fraction of observed isoprene mixing ratios, which may include advected pollution, was estimated using the equation from Langford et al. (2010b), which estimated a 30 and 20 % contribution in August and September respectively. These values were significantly higher than for iso-pentane, a non-biogenic compound, to which the same analysis was applied. The temperature dependent component of isoprene in October, November and December showed no significant difference to that of iso-pentane, suggesting the biogenic component was reduced or absent at lower temperatures. High correlations of m/z 69 with light and temperature during August and September indicate that isoprene was the likely major component during these months, however the rest of the period the contribution of other compounds such as furan and other alkenes at that mass may have increased, thereby overestimating the isoprene signal (Yuan et al., 2014).

3.1.3 Modelling the biogenic isoprene contribution in London

An attempt was made to model the biogenic isoprene component during August and September using the light and temperature algorithms of Guenther et al. (1995), hereafter termed G95. The foliar emissions based model calculates VOC fluxes as follows;

$$F = D \times \varepsilon \times \gamma, \tag{5}$$

where D is the foliar density ($\mathrm{kg\,dry\,matter\,m^{-2}}$), ε is an ecosystem dependent base emission rate ($\mathrm{\mu g\,C\,m^{-2}\,s^{-1}}$ normalised to a PAR flux of $1000\,\mathrm{\mu mol\,m^{-2}\,s^{-1}}$ and leaf temperature of $303.15\,\mathrm{K}$), and γ is a dimensionless activity adjustment factor accounting for the effects of PAR and leaf temperature. Ambient air temperature and PAR measurements were used to calculate the light and temperature controlled parameters C_L and C_T for γ, where,

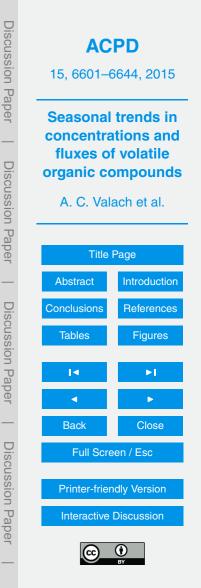$$\gamma = C_L \times C_T \tag{6}$$

The slope of the linear regression of the measured total isoprene flux and γ provided an emission factor in mg m^{-2} h^{-1}, which was converted to µg g^{-1} h^{-1} by dividing by the foliar density D (129 g m^{-2}). The foliar density was estimated using the total leaf area as seen from visible satellite imagery within the flux footprint (approx. 9 %) and leaf dry weight for representative species commonly planted in the area such as *Platanus x acerifolia* (City of Westminster, 2009), which are also high isoprene emitters (Geron et al., 1994). The resulting base emission rate ε from the measured fluxes was 6.5 µg g^{-1} h^{-1} which compares well with the figure given in the literature (5 µg g^{-1} h^{-1}) for cities in a cool climate (Guenther et al., 1995). These estimates are representative of the biogenic isoprene fluxes from a highly heterogeneous canopy within the flux footprint, including both high and low isoprene emitting species as well as low average foliar density due to the sparse distribution of urban roadside and park trees. Figure 5 shows that the modelled isoprene fluxes using the calculated base emission rate by wind direction compared well with the measured fluxes. Linear regressions from wind directions that have a strong anthropogenic component are lower, e.g. W ($R^2 = 0.13$, $p < 0.001$), than areas dominated by biogenic sources, e.g. SE ($R^2 = 0.81$, $p < 0.001$) with the nearby Temple Gardens. Modelled fluxes seemingly underestimated observed isoprene fluxes since these included the traffic component, however it appears that biogenic isoprene represents a detectable source contribution in summer.

3.2   VOC/VOC correlations and ratios

VOC/VOC correlations for fluxes indicated ($R^2 = 0.40$ and 0.62, $p < 0.001$) compounds with non-traffic sources had higher correlations (R^2 between 0.40–0.62, $p < 0.001$). VOC/VOC correlations for concentrations (R^2 between 0.13–0.84, $p < 0.001$) showed highest correlations between traffic related compounds (R^2 between 0.45–0.84, $p < 0.001$) and between the oxygenated compounds and isoprene (R^2 between 0.55–0.69, $p < 0.001$) (Fig. 6). Higher correlations between oxygenated VOCs could indicate source commonality or formation mechanisms that depend on similar environmental factors. Scatterplots between aromatic compounds and isoprene/oxygenated
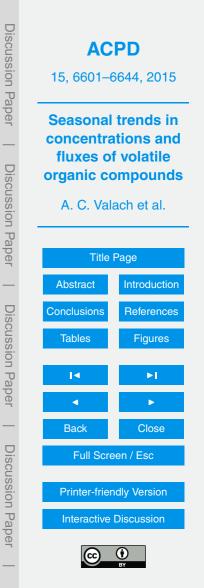
compounds tended to show bimodal distributions indicating separate source contributions (Fig. 6, left panel). Using temperature or, to a smaller extent, PAR as a third variable highlights a temperature or light dependency of the second source supporting the existence of additional biogenic and/or atmospheric sources. In the example of isoprene against benzene the relationship changes with temperature from 2 : 1 to 1 : 2.

3.2.1 Benzene to toluene ratios

Benzene to toluene (b/t) ratios can help identify source types and changes in ratios can indicate the photochemical age of an air mass as toluene reacts at a faster rate with OH in the atmosphere, assuming sufficient OH concentrations to drive the reaction (Warneke et al., 2007). Median (IQR) b/t ratios were 0.21 (0.02–0.43) for fluxes and 0.45 (0.39–0.48) for concentrations respectively and are comparable to those reported in the literature (Heeb et al., 2000; Langford et al., 2009; Valach et al., 2014). Individual maxima and minima were seen in the b/t concentration ratios, examples of which are discussed below. Traffic related emissions are considered to be an important source of benzene and toluene in London with a b/t exhaust emission ratio of 0.4 based on derived yearly emissions (Zavala et al., 2006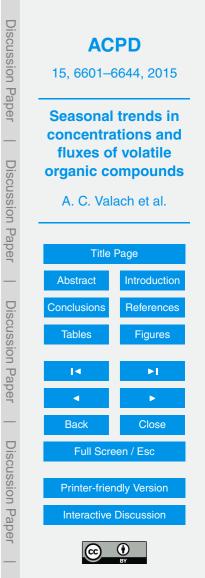) and measurements ranging from 0.32 to 0.65 (Rogers et al., 2006). Airborne flux measurements have shown average b/t flux ratios of 0.31 with lower ratios of 0.07 to 0.1 over industrial areas due to increased toluene emissions from industrial processes (Karl et al., 2009; Velasco et al., 2007). Average observed b/t concentration ratios of 0.26 (Karl et al., 2009), 0.25 (Rogers et al., 2006) and 0.20 (Velasco et al., 2007) have been observed in other megacities. Observed b/t concentration ratios agreed with the assumed 0.4 traffic related emission ratio, however b/t flux ratios were lower. Evaporative emissions from gasoline or direct industrial toluene emissions may have contributed to the lower b/t flux ratios. Furthermore, b/t concentration ratios from diesel emissions of 0.26 have been reported (Corrêa and Arbilla, 2006). The widespread use of diesel fuel in London (buses, taxis and some trains) and diesel emissions from roads exclusively permitting buses and taxis, such as Oxford Street (approx. 1.3 km W from the measurement site) or central

Title Page

Abstract | Introduction

Conclusions | References

Tables | Figures

|◀ | ▶|

◀ | ▶

Back | Close

Full Screen / Esc

Printer-friendly Version

Interactive Discussion

railway nodes, such as Waterloo Train Station (1 km to the S), may have affected b/t ratios. Wind speed and direction can play a role for b/t concentration ratios by transporting pollution over longer distances allowing more time or exposure to higher OH concentrations, thus increasing the ratio. An example of this was seen on the 12 August when median (IQR) b/t concentration ratios reached 0.5 (0.45–0.56) with stronger SE winds (mean $3.67 \, \text{m s}^{-1}$) possibly advecting pollution from Benelux/Northern Europe, whereas on the 9 August median b/t ratios were 0.34 (0.30–0.38) with low wind speeds (mean $1.28 \, \text{m s}^{-1}$) indicating higher contributions of local sources (i.e. 60 % London influence) (Bohnenstengel et al., 2014). On both days OH concentrations above London were around 1.25×10^6 molecules cm^{-3} and b/t flux ratios were not significantly different making pollution advection a likely cause of the observed difference (L. Whalley, personal communication 2014). Calculated back trajectories using the HYSPLIT trajectory model (Hybrid Single Particle Lagrangian Integrated Trajectory Model, Draxler and Rolph, 2014) were run at 3 h intervals starting at ground-level (10 m) from London and propagated 24 h backwards in time. These agreed with the changes in measured b/t ratios (Fig. 7) and during episodes of high b/t ratios indicated that air masses passed over continental Europe within the past day which could have entrained pollution. The median monthly b/t flux ratio stayed between 0.18 and 0.26 which is to be expected since only local fluxes were detected, however the median (IQR) monthly b/t ratio for concentrations steadily increased from 0.41 (0.36–0.47) to 0.62 (0.55–0.70) from August to December. Assuming less local photochemical removal during the winter months, as OH concentrations in London are often below the detection limit during winter (Bohnenstengel et al., 2014), this implies advected pollution from mainland Europe may be common in winter or biomass burning may play a greater role in colder months, as this is associated with higher b/t ratios, e.g. 1.67 (Lemieux et al., 2004), due to the different fuel combustion emission profile.

Median (IQR) concentration ratios for benzene to C_2-benzenes were 0.31 (0.28–0.33) and toluene to C_2-benenes were 0.72 (0.63–0.81), which both agree with pre-
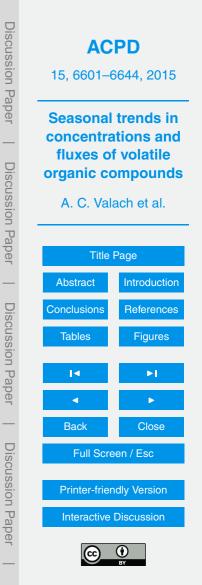
vious values and suggest that these masses are indeed the ascribed traffic related compounds (Heeb et al., 2000; Warneke et al., 2001).

3.2.2 VOC to CO_2 correlations and ratios

Correlations of VOC with CO_2 fluxes measured concurrently on site were low (R^2 = 0.06–0.21, $p < 0.001$), but mostly comparable with values from a previous study in London, which ranged from R^2 = 0.09–0.26 (Harrison et al., 2012). In this study acetaldehyde showed the highest and isoprene was among the lowest correlations with CO_2 fluxes, which is opposite to the Harrison et al. study. This may indicate in the case of acetaldehyde increased and for isoprene reduced source commonality with CO_2 during the respective measurement periods. Concentration correlations were highest for traffic related compounds (R^2 = 0.25–0.44, $p < 0.001$) and lower with the other compounds ($R^2 < 0.11$, $p < 0.05$) with acetone showing no significant relationship ($p = 0.88$). Most compound flux and concentration correlations with CO_2 significantly increased towards December ($R^2 \leq 0.49$ and ≤ 0.86, respectively) reflecting the increased commonality of combustion sources towards winter. Only correlations with C_2-benzene fluxes declined in November and December.
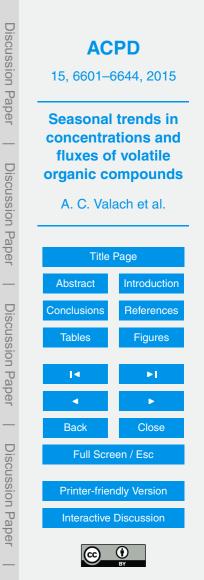
Median VOC/CO_2 flux ratios ranged from 0.05 to 0.26 with isoprene and benzene showing low ratios and toluene and C_2-benzenes high ratios. Highest flux ratios were with W winds, whereas lowest for biogenic compounds with N and for traffic related compounds S wind directions. Flux ratios declined towards December as CO_2 fluxes increased and VOC fluxes decreased. Similarly, VOC/CO_2 concentration ratios were between 0.45×10^{-6} and 14.6×10^{-6} (ppb/ppb) with isoprene and benzene representing the lowest and methanol and acetone the highest ratios. Highest concentration ratios were in August for oxygenated compounds/isoprene and December for traffic-related species.

3.3 Wind direction and flux footprint analysis

Polar Annulus and Polar plots were constructed for VOC fluxes and mixing ratios respectively and representative compounds are shown (Fig. 8). Polar plots use a generalized additive model (GAM) to interpolate between wind direction and wind speed averaged data points within the OpenAir package in R (see Wood, 2006; Hastie and Tibshirani, 1990; Carslaw and Ropkins, 2012). Polar Annulus plots averaged by time of day instead of wind speed show diurnal variability with wind direction. The majority of the time (83 %) unstable and near neutral conditions prevailed ($\zeta < 0.2$), although the frequency varied between months with 87, 89, 82, 84 and 69 % during August, September, October, November and December, respectively. Wind direction with mostly unstable conditions were with W and S winds and near neutral with N or E winds. Mixing ratios were on average highest with low wind speeds (showing a negative correlation) when pollutants accumulate due to reduced mixing, indicating local emissions (Fig. 8, bottom). Largest fluxes for all compounds were from the NW with either one daytime peak (e.g. isoprene) or two distinct rush hour peaks (e.g. benzene) (Fig. 8, top). On average fluxes were largest from the W > E ≥ N > S (F statistic between 60.37 and 227.06, $p < 0.001$) because of increased emission rates of specific compound sources. Separated by month, fluxes were largest from W > N > E ≥ S in August and September whereas during October, November and December fluxes followed the pattern W > E ≥ N > S. Due to the relatively low measurement height the flux footprint was limited to the immediate surrounding area allowing close coupling with the surface layer and similar surface roughness. The average length of the maximum flux footprint contribution (X_{max}) was around 330 m and 90 % of all the fluxes (X_{90}) originated from within 900 m. The median footprint area was 1.8 km^2. This established that the majority of emission sources contributing to the measured fluxes must have been local. Additionally, the selected emission grid (cf Sect. 2.3.1 above) encompassed 97 % of the footprint with S and W wind directions, but only 80 and 84 % during E and N winds. Grid square 5 represented the maximum contribution area since

Title Page

Abstract | Introduction

Conclusions | References

Tables | Figures

|◄ | ►|

◄ | ►

Back | Close

Full Screen / Esc

Printer-friendly Version

Interactive Discussion

it encompassed the measurement point. Average footprint contributions (mean ± SD) comprised of grid squares 1 (2 ± 4 %), 2 (5 ± 7 %), 4 (4 ± 5 %) and 5 (52 ± 31 %) during S and W wind conditions, squares 6 (4 ± 9 %) and 9 (4 ± 10 %) indicated E wind conditions, and square 8 (18 ± 27 %) N wind conditions. During October contributions from square 9 increased to 10 % and were more frequent at 30 % in December. Squares 3 (0.6 ± 2 %) and 7 (0.9 ± 2 %) provided minimal average contributions.

Green areas, as defined on the OS map, within the grid were evenly distributed across the 9 km^2 and comprised 8.8 % of the total grid area, half of which was captured by the National Forest Inventory England (NFI, 2012). This definition excluded individual trees in parks and avenues, which can encompass up to 50 % of trees maintained by the council in central London (City of Westminster, 2009). Only grid square 1 included a large green area of 23 ha (St. James' Park).

Since footprints were relatively small it is possible that the Thames River to the S caused the low fluxes associated with S winds (i.e. squares 1, 2 and 3). For traffic related compound fluxes there were statistically significant contributions from the W (i.e. squares 4, 5, and 7), followed by the N (square 8) and E (squares 6 and 9) likely from the nearby heavily trafficked roads (Kingsway, Charing Cross, Strand and Blackfriars areas, respectively). For isoprene, and to some degree methanol and acetaldehyde, fluxes were highest from the W and E with green areas being within the maximum contributing distance (X_{max}) of the footprint (300 m). Correlations of grid square contributions in the footprint with fluxes can also give information on grid square emission rates. Generally positive correlations with fluxes across most compounds were seen from the W (squares 4, 5 and 7) confirming that increased emissions from these grid squares were driving the high fluxes, although these were largest ($R = 0.40$–0.46, $p < 0.001$) during October and November, especially for masses associated with biogenic sources (m/z 33, 45, 59 and 69). Square 8 showed positive correlations for benzene and only in August for all compounds.

Highest mixing ratios with wind direction were from E > N ≥ W > S for traffic related compounds, whereas oxygenated compounds/isoprene followed a similar pattern as

the fluxes of W ≥ E > N ≥ S (*F* statistic: 47.49–86.95, *p* < 0.001). Easterly winds in London are often associated with synoptic conditions that bring European Continental air masses to the UK, resulting in higher background concentrations. Furthermore, since the boundary layer was on average more stably stratified with E wind conditions, it is likely that pollutant concentrations were allowed to build up resulting in the observed higher concentrations to the E for the more ubiquitous compounds, whereas concentrations of compounds with biogenic contributions additionally had strong source areas to the W, such as several parks (St. James' Park, Hyde Park and Regents Park, total 331 ha).

3.4   Comparisons with London and National Atmospheric Emissions Inventories

The London (LAEI) and National Atmospheric Emissions Inventories (NAEI) produce biannual emission estimates for a range of pollutants and emission sources. Total VOC emission estimates are provided, but only benzene and 1,3-butadiene are listed separately. Measured emissions were compared with annual estimated emissions for the above OS grid area from 2012 for benzene using the LAEI and indirectly speciated VOCs of the NAEI. Using the average flux footprint, the grid square estimates were compared with the scaled flux measurements from the equivalent area.

LAEI emission estimates included contributions from major (69 %) and minor roads (4 %), as well as evaporative emissions (27 %) (LAEI, 2012). No data were available on cold start emissions for benzene. The calculated standard errors provided some uncertainty approximation. Measured fluxes compared well with emission estimates, although the LAEI predicted slightly smaller benzene fluxes (Fig. 9). Comparisons of fluxes with wind directions (Sect. 3.3) agreed well with the LAEI emission estimates for the respective grid squares with highest emissions from squares 4, 5, 7 and 8 (i.e. W and N directions). This comparison assumes that the benzene fluxes during the measurement period were representative of annual emissions with any significant seasonal
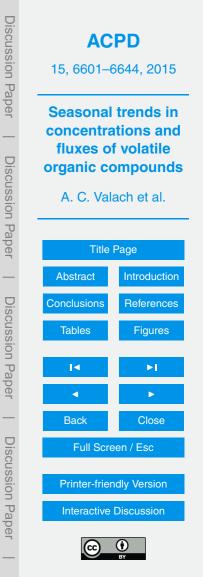
variation in benzene emission rates captured in this five month period. Section 3.1.2 confirmed that there was little month-to-month variability in the benzene flux.

Using speciated VOC emission contributions (% of total VOC emissions) for 2006 (NAEI Reference: 45321001/0/AO6069/NP) and emission maps from 2012 for total non-methane VOC emissions, speciated estimates could be compared with observations (Fig. 9). NAEI includes a wider range of emission sources divided into 11 SNAP sectors including industrial, commercial and residential processes, transport, waste treatment, solvent use, point sources, agriculture and nature, although the latter two were unavailable for the London urban area. NAEI estimates for benzene exceed the LAEI due to the inclusion of a wider range of sources beyond traffic related emissions. Sum C_2-benzene emission estimates consisted of ethyl benzene, (m + p)-xylene and o-xylene. Benzene and methanol emissions agreed very well, however for all the other compounds estimated emissions were significantly lower than the measured fluxes. Uncertainties related to the measurements, such as isobaric interferences within the PTR-MS could have contributed to measurement overestimation, whereas uncertainties within the emissions estimates and the use of older speciation values may have impacted the estimates. In the case of isoprene, only minimal emissions are estimated which do not include the biogenic sources that contributed to the measured fluxes. It is also likely that some of the m/z 69 signal could be attributed to cyclic alkenes, but Sect. 3.1.3 showed that biogenic isoprene provided a significant contribution during August and September in central London.

4 Conclusion

Vehicle emissions have been shown to be the dominant source of VOC fluxes and concentrations in central London, although biogenic sources and secondary atmospheric formation may have provided a significant contribution, particularly in August and September. There were observable spatial and temporal variations in relative source impacts at different resolutions such as hour to month. The measured VOC
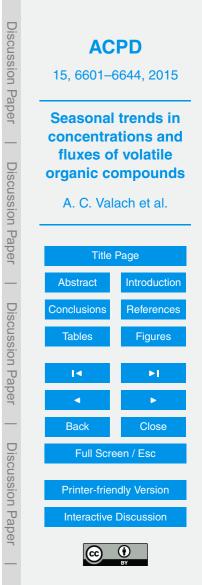
fluxes originated from an area within a 1 km radius around the measurement site and some instances of pollution advection were seen to affect concentrations, but many of the spatio-temporal differences in the observed mixing ratios were attributable to emissions and boundary layer dynamics.

The biogenic component of isoprene was modelled using the G95 algorithm and the calculated base emission rate closely matched previous values for urban areas. Quantifying the biogenic signal of VOCs in urban areas with a high percentage of parklands can greatly aid in understanding photochemical pollution precursor emissions and improve predictions of high pollution episodes.

Close agreement between the flux footprint contributions and the LAEI for benzene emissions, a compound which is thought to be accurately estimated in the inventory but associated with high measurement uncertainty, gives confidence in the PTR-MS measurements. Good agreement was also seen with methanol estimated from the NAEI, however other compounds were all greatly underestimated in the emissions inventory. This provides further evidence for successful implementation of VOC flux measurements in heterogeneous urban landscapes when measurement sites fulfil basic eddy covariance criteria. Further VOC flux observations are essential to help identify major source components for a range of VOCs which can be included in emissions inventories.

References

Andreae, M. O. and Merlet, P.: Emission of trace gases and aerosols from biomass burning, Global Biogeochem. Cy., 15, 955–966, doi:10.1029/2000GB001382, 2001.

Atkinson, R.: Atmospheric chemistry of VOCs and NO_x, Atmos. Environ., 34, 2063–2101, doi:10.1016/S1352-2310(99)00460-4, 2000.

Bohnenstengel, S. I., Belcher, S. E., Allan, J. D., Allen, G., Bacak, A., Bannan, T. J., Barlow, J. F., Beddows, D. C. S., Bloss, W. J., Booth, A. M., Chemel, C., Coceal, O., Di Marco, C. F., Faloon, K. H., Fleming, Z. L., Furger, M., Geitl, J. K., Graves, R. R., Green, D. C., Grimmond, C. S. B., Halios, C., Hamilton, J. F., Harrison, R. M., Heal, M. R., Heard, D. E., Helfter, C., Herndon, S. C., Holmes, R. E., Hopkins, J. R., Jones, A. M., Kelly, F. J., Kotthaus, S., Langford, B., Lee, J. D., Leigh, R. J., Lewis, A. C., Lidster, R. T., Lopez-Hilfiker, F. D., McQuaid, J. B., Mohr, C., Monks, P. S., Nemitz, E., Ng, N. L., Percival, C. J., Prévôt, A. S. H., Ricketts, H. M. A., Sokhi, R., Stone, D., Thornton, J. A., Tremper, A. H., Valach, A. C., Visser, S., Whalley, L. K., Williams, L. R., Xu, L., Young, D. E., and Zotter, P.: Meteorology, air quality, and health in London: the ClearfLo project, B. Am. Meteorol. Soc., doi:10.1175/BAMS-D-12-00245.1, in press, 2015.

Carslaw, D. C. and Ropkins, K.: Openair – an R package for air quality data analysis, Environ. Modell. Softw., 27, 52–61, 2012.

City of Westminster: Trees and the Public Realm (Draft), City of Westminster, City Planning Delivery Unit, London, 2009.

Clarke, J. U.: Evaluation of censored data methods to allow statistical comparisons among very small samples with below detection limit observations, Environ. Sci. Technol., 32, 177–183, 1998.

Corrêa, S. M. and Arbilla, G.: Aromatic hydrocarbons emissions in diesel and biodiesel exhaust, Atmos. Environ., 40, 6821–6826, 2006.
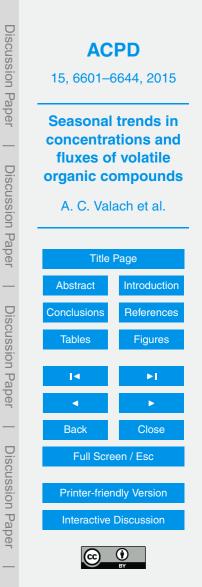
de Gouw, J. A.: Budget of organic carbon in a polluted atmosphere: results from the New England air quality study in 2002, J. Geophys. Res., 110, D16305, doi:10.1029/2004JD005623, 2005.

de Gouw, J. A. and Warneke, C.: Measurements of volatile organic compounds in the earth's atmosphere using proton-transfer-reaction mass spectrometry, Mass Spectrom. Rev., 26, 223–257, 2007.

Department for Transport: Traffic count data for the City of London, available at: http://www.dft.gov.uk/traffic-counts/area.php?region=London, (last access: 5 August 2014), 2014.

Draxler, R. R. and Rolph, G. D.: HYSPLIT (HYbrid Single–Particle Lagrangian Integrated Trajectory) Model, available at: http://www.arl.noaa.gov/HYSPLIT_info.php(last access: 13 August 2014), retrieved 12 September 2014, from NOAA ARL READY, 2008.

Foken, T. and Wichura, B.: Tools for quality assessment of surface-based flux measurements, Agr. Forest Meteorol., 78, 83–105, doi:10.1016/0168-1923(95)02248-1, 1996.

Foken, T., Göckede, M., Mauder, M., Mahrt, L., Amiro, B., and Munger, W.: Post-field data quality control, in: Handbook of Micrometeorology, edited by: Lee, X. M., Kluwer Academic Publishers, Dordrecht, the Netherlands, 181–208, 2004.

Garrat, J.: The Atmospheric Boundary Layer, Cambridge University Press, Cambridge, UK, 1992.

Geron, C. D., Guenther, A. B., and Pierce, T. E.: An improved model for estimating emissions of volatile organic compounds from forests in the eastern United States, J. Geophys. Res.-Atmos., 99, 12773–12791, 1994.

Guenther, A., Hewitt, C. N., Erickson, D., Fall, R., Geron, C., Graedel, T., Harley, P., Klinger, L., Lerdau, M., McKay, W. A., Pierce, T., Scholes, B., Steinbrecher, R., Tallamra, R., Taylor, J., and Zimmerman, P.: A global model of natural volatile organic compound emissions, J. Geophys. Res., 100, 8873–8892, doi:10.1029/94JD02950, 1995.

Harley, R. A. and Cass, G. R.: Modeling the concentrations of gas–phase toxic organic air pollutants?: direct emissions and atmospheric formation, Environ. Sci. Technol., 28, 88–98, 1994.

Harrison, R. M., Dall'Osto, M., Beddows, D. C. S., Thorpe, A. J., Bloss, W. J., Allan, J. D., Coe, H., Dorsey, J. R., Gallagher, M., Martin, C., Whitehead, J., Williams, P. I., Jones, R. L., Langridge, J. M., Benton, A. K., Ball, S. M., Langford, B., Hewitt, C. N., Davison, B., Martin, D., Petersson, K. F., Henshaw, S. J., White, I. R., Shallcross, D. E., Barlow, J. F., Dunbar, T., Davies, F., Nemitz, E., Phillips, G. J., Helfter, C., Di Marco, C. F., and Smith, S.: Atmospheric chemistry and physics in the atmosphere of a developed megacity (London): an overview of the REPARTEE experiment and its conclusions, Atmos. Chem. Phys., 12, 3065–3114, doi:10.5194/acp-12-3065-2012, 2012.

Hastie, T. J. and Tibshirani, R.: Generalized Additive Models, Chapman and Hall, London, 1990.
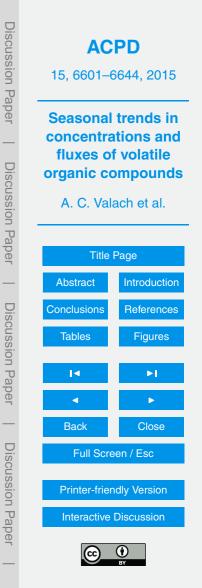
Hayward, S., Hewitt, C. N., Sartin, J. H., and Owen, S. M.: Performance characteristics and applications of a proton transfer reaction-mass spectrometer for measuring volatile organic compounds in ambient air, Environ. Sci. Technol., 36, 1554–1560, 2002.

Heeb, N. V, Forss, A., Bach, C., Reimann, S., Herzog, A., and Ja, H. W.: A comparison of benzene, toluene and C-benzenes mixing ratios in automotive exhaust and in the suburban atmosphere during the introduction of catalytic converter technology to the Swiss Car Fleet, Atmos. Environ., 34, 3103–3116, 2000.

Helfter, C., Famulari, D., Phillips, G. J., Barlow, J. F., Wood, C. R., Grimmond, C. S. B., and Nemitz, E.: Controls of carbon dioxide concentrations and fluxes above central London, Atmos. Chem. Phys., 11, 1913–1928, doi:10.5194/acp-11-1913-2011, 2011.

Helsel, D. R. and Hirsch, R. M.: Statistical Methods in Water Resources, Elsevier, New York, 1992.

Hewitt, C. N., Hayward, S., and Tani, A.: The application of proton transfer reaction-mass spectrometry (PTR-MS) to the monitoring and analysis of volatile organic compounds in the atmosphere, J. Environ. Monitor., 5, 1–7, doi:10.1039/b204712h, 2003.

Horst, T. W.: A simple formula for attenuation of eddy fluxes measured with first-order-response scalar sensors, Bound.-Lay. Meteorol., 82, 219–233, 1997.

Kansal, A.: Sources and reactivity of NMHCs and VOCs in the atmosphere: a review, J. Hazard. Mater., 166, 17–26, doi:10.1016/j.jhazmat.2008.11.048, 2009.

Karl, T. G., Spirig, C., Rinne, J., Stroud, C., Prevost, P., Greenberg, J., Fall, R., and Guenther, A.: Virtual disjunct eddy covariance measurements of organic compound fluxes from a subalpine forest using proton transfer reaction mass spectrometry, Atmos. Chem. Phys., 2, 279–291, doi:10.5194/acp-2-279-2002, 2002.

Title Page

Abstract | Introduction

Conclusions | References

Tables | Figures

|◄ | ►|

◄ | ►

Back | Close

Full Screen / Esc

Printer-friendly Version

Interactive Discussion

Karl, T., Apel, E., Hodzic, A., Riemer, D. D., Blake, D. R., and Wiedinmyer, C.: Emissions of volatile organic compounds inferred from airborne flux measurements over a megacity, Atmos. Chem. Phys., 9, 271–285, doi:10.5194/acp-9-271-2009, 2009.

Kim, Y. M., Harrad, S., and Harrison, R. M.: Concentrations and sources of VOCs in urban domestic and public microenvironments, Environ. Sci. Technol., 35, 997–1004, 2001.

Kljun, N., Calanca, P., Rotachhi, M. W., and Schmid, H. P.: A simple parameterisation for flux footprint predictions, Bound.-Lay. Meteorol., 112, 503–523, 2004.

Kormann, R. and Meixner, F. X.: An analytical footprint model for non-neutral stratification, Bound.-Lay. Meteorol., 99, 207–224, 2001.

Kotthaus, S. and Grimmond, C. S. B.: Identification of micro-scale anthropogenic CO_2, heat and moisture sources – processing eddy covariance fluxes for a dense urban environment, Atmos. Environ., 57, 301–316, doi:10.1016/j.atmosenv.2012.04.024, 2012.

Kotthaus, S. and Grimmond, C. S. B.: Energy exchange in a dense urban environment – Part II: Impact of spatial heterogeneity of the surface, Urban Climate, 10, 1–27, doi:10.1016/j.uclim.2013.10.001, 2013.

LAEI, London Atmospheric Emission Inventory, LAEI database 2012, available at: http://www.cleanerairforlondon.org.uk/londons-air/air-quality-data/london-emissions-laei/road-traffic-emissions (last access: 19 September 2014), 2013.

Lamsal, L. N., Martin, R. V., Padmanabhan, A., van Donkelaar, A., Zhang, Q., Sioris, C. E., Chance, K., Kurosu, T. P., and Newchurch, M. J.: Application of satellite observations for timely updates to global anthropogenic NO_x emission inventories, Geophys. Res. Lett., 38, L05810, doi:10.1029/2010GL046476, 2011.

Langford, B., Davison, B., Nemitz, E., and Hewitt, C. N.: Mixing ratios and eddy covariance flux measurements of volatile organic compounds from an urban canopy (Manchester, UK), Atmos. Chem. Phys., 9, 1971–1987, doi:10.5194/acp-9-1971-2009, 2009.

Langford, B., Misztal, P. K., Nemitz, E., Davison, B., Helfter, C., Pugh, T. A. M., MacKenzie, A. R., Lim, S. F., and Hewitt, C. N.: Fluxes and concentrations of volatile organic compounds from a South-East Asian tropical rainforest, Atmos. Chem. Phys., 10, 8391–8412, doi:10.5194/acp-10-8391-2010, 2010a.

Langford, B., Nemitz, E., House, E., Phillips, G. J., Famulari, D., Davison, B., Hopkins, J. R., Lewis, A. C., and Hewitt, C. N.: Fluxes and concentrations of volatile organic compounds above central London, UK, Atmos. Chem. Phys., 10, 627–645, doi:10.5194/acp-10-627-2010, 2010b.

Title Page

Abstract | Introduction

Conclusions | References

Tables | Figures

|◀ | ▶|

◀ | ▶

Back | Close

Full Screen / Esc

Printer-friendly Version

Interactive Discussion

Langford, B., Acton, W., Ammann, C., Valach, A. C., and Nemitz, E.: Eddy-covariance data with low signal-to-noise ratio: time-lag determination, uncertainties and limit of detection, Atmos. Meas. Tech., in review, 2015.

Lemieux, P. M., Lutes, C. C., and Santoianni, D. A.: Emissions of organic air toxics from open burning: a comprehensive review, Prog. Energ. Combust., 30, 1–32, 2004.
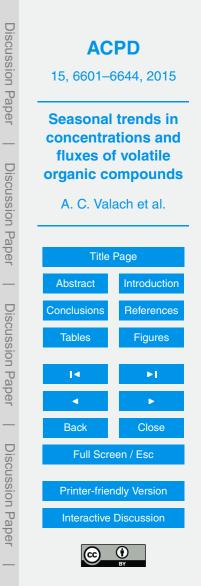
Lindinger, W., Hansel, A., and Jordan, A.: On-line monitoring of VOCs at pptv levels by means of PTR-MS, medical applications, food control and environonmental research, Int. J. Mass Spectrom., 173, 191–241, doi:10.1016/0015-1882(95)90197-3, 1998.

Lipari, F., Dasch, J. M., and Scruggs, W. F.: Aldehyde emissions from wood-burning fireplace, Environ. Sci. Technol., 18, 326–330, 1984.

Met Office UK: UK Climate summaries, available at: http://www.metoffice.gov.uk/climate/uk/summaries/2012 (last access: 9 October 2013), 2013.

Moncrieff, J., Finnigan, R. C. J., and Meyers, T.: Averaging, detrending, and filtering of eddy covariance time series, in: Handbook of Micrometeorology, edited by: Lee, W. M., Kluwer Academic Publishers, Dordrecht, 7–30, 2004.

NAEI, National Atmospheric Emission Inventory: available at: http://naei.defra.gov.uk/data/ (last access: 10 October 2014), 2006.

National Forest Inventory England: available at: http://www.forestry.gov.uk/forestry/hcou-54pg9u (last access: 21 September 2014), 2012.

Neftel, A., Spirig, C., and Ammann, C.: Application and test of a simple tool for operational footprint evaluations, Environ. Pollut., 152, 644–652, doi:10.1016/j.envpol.2007.06.062, 2008.

Nemitz, E., Hargreaves, K. J., McDonald, A. G., Dorsey, J. R., and Fowler, D.: Meteorological measurements of the urban heat budget and CO_2 emissions on a city scale, Environ. Sci. Technol., 36, 3139–3146, 2002.

Oke, T. R.: Towards better scientific communication in urban climate, Theor. Appl. Climatol., 84, 179–190, 2006.

Palmer, P. I., Abbot, D. S., Fu, T.-M., Jacob, D. J., Chance, K., Kurosu, T. P., Guenther, A., Wiedinmyer, C., Stanton, J. C., Pilling, M. J., Pressley, S. N., Lamb, B., and Sumner, A. L.: Quantifying the seasonal and interannual variability of North American isoprene emissions using satellite observations of the formaldehyde column, J. Geophys. Res., 111, D12315, doi:10.1029/2005JD006689, 2006.

Seasonal trends in concentrations and fluxes of volatile organic compounds

A. C. Valach et al.

Title Page

Abstract | Introduction

Conclusions | References

Tables | Figures

|◄ | ►|

◄ | ►

Back | Close

Full Screen / Esc

Printer-friendly Version

Interactive Discussion

Park, C., Schade, G. W., and Boedeker, I.: Flux measurements of volatile organic compounds by the relaxed eddy accumulation method combined with a GC-FID system in urban Houston, Texas, Atmos. Environ., 44, 2605–2614, doi:10.1016/j.atmosenv.2010.04.016, 2010.

Park, C., Schade, G. W., and Boedeker, I.: Characteristics of the flux of isoprene and its oxidation products in an urban area, J. Geophys. Res., 116, D21303, doi:10.1029/2011JD015856, 2011.

Rogers, T. M., Grimsrud, E. R., Herndon, S. C., Jayne, J. T., Kolb, C. E., Allwine, E., Westberg, H., Lamb, B. K., Zavala, M.,Molina, L. T., Molina, M. J., and Knighton, W. B.: On-road measurements of volatile organic compounds in the Mexico City metropolitan area using proton transfer reaction mass spectrometry, Int. J. Mass Spectrom., 252, 26–37, 2006.

Schade, G. W. and Goldstein, A. H.: Fluxes of oxygenated volatile organic compounds from a ponderosa pine plantation, J. Geophys. Res., 106, 3111–3123, 2001.

Singh, H. B., O'Hara, D., Herlth, D., Sachsse, W., Blake, D. R., Bradshaw, J. D., Kanakidou, M., and Crutzen, P. J.: Acetone in the atmosphere: distribution, source, and sinks, J. Geophys. Res., 99, 1805–1819, 1994.

Spirig, C., Neftel, A., Ammann, C., Dommen, J., Grabmer, W., Thielmann, A., Schaub, A., Beauchamp, J., Wisthaler, A., and Hansel, A.: Eddy covariance flux measurements of biogenic VOCs during ECHO 2003 using proton transfer reaction mass spectrometry, Atmos. Chem. Phys., 5, 465–481, doi:10.5194/acp-5-465-2005, 2005.

Srivastava, A., Sengupta, B., and Dutta, S. A.: Source apportionment of ambient VOCs in Delhi City, Sci. Total Environ., 343, 207–220, 2005.

Taipale, R., Ruuskanen, T. M., Rinne, J., Kajos, M. K., Hakola, H., Pohja, T., and Kulmala, M.: Technical Note: Quantitative long-term measurements of VOC concentrations by PTR-MS – measurement, calibration, and volume mixing ratio calculation methods, Atmos. Chem. Phys., 8, 6681–6698, doi:10.5194/acp-8-6681-2008, 2008.

Valach, A. C., Langford, B., Nemitz, E., MacKenzie, A. R., and Hewitt, C. N.: Concentrations of selected volatile organic compounds at kerbside and background sites in central London, Atmos. Environ., 95, 456–467, doi:10.1016/j.atmosenv.2014.06.052, 2014.

Velasco, E., Lamb, B., Pressley, S., Allwine, E., Westberg, H., and Jobson, B. T.: Flux measurements of volatile organic compounds from an urban landscape, Geophys. Res. Lett., 32, 2–5, doi:10.1029/2005GL023356, 2005.

Velasco, E., Lamb, B., Westberg, H., Allwine, E., Sosa, G., Arriaga-Colina, J. L., Jobson, B. T., Alexander, M. L., Prazeller, P., Knighton, W. B., Rogers, T. M., Grutter, M., Herndon, S. C.,

Kolb, C. E., Zavala, M., de Foy, B., Volkamer, R., Molina, L. T., and Molina, M. J.: Distribution, magnitudes, reactivities, ratios and diurnal patterns of volatile organic compounds in the Valley of Mexico during the MCMA 2002 & 2003 field campaigns, Atmos. Chem. Phys., 7, 329–353, doi:10.5194/acp-7-329-2007, 2007.

Velasco, E., Pressley, S., Grivicke, R., Allwine, E., Coons, T., Foster, W., Jobson, B. T., Westberg, H., Ramos, R., Hernández, F., Molina, L. T., and Lamb, B.: Eddy covariance flux measurements of pollutant gases in urban Mexico City, Atmos. Chem. Phys., 9, 7325–7342, doi:10.5194/acp-9-7325-2009, 2009.

Warneke, C., van der Veen, C., de Gouw, J. A., and Kok, A.: Measurements of benzene and toluene in ambient air using proton-transfer-reaction mass spectrometry?: calibration, humidity dependence, and field intercomparison, Int. J. Mass Spectrom., 207, 167–182, 2001.

Warneke, C., de Gouw, J. A., Kuster, W. C., Goldan, P. D., and Fall, R.: Validation of atmospheric VOC measurements by proton-transfer-reaction mass spectrometry using a gaschromatographic pre-separation method, Environ. Sci. Technol., 37, 2494–2501, 2003.

Warneke, C., McKeen, S. A., de Gouw, J. A., Goldan, P. D., Kuster, W. C., Holloway, J. S., Williams, E. J., Lerner, B. M., Parrish, D. D., Trainer, M., Fehsenfeld, C., Kato, S., Atlas, E. L., Baker, A., and Blake, D. R.: Determination of urban volatile organic compound emission ratios and comparison with an emissions database, J. Geophys. Res., 112, D10S47, doi:10.1029/2006JD007930, 2007.

Wood, S.: Generalized Additive Models: An Introduction with R, Chapman and Hall/CRC, Boca Raton, FL, USA, 2006.

Yuan, B., Warneke, C., Shao, M., and de Gouw, J. A.: Interpretation of volatile organic compound measurements by proton-transfer-reaction mass spectrometry over the deepwater horizon oil spill, Int. J. Mass Spectrom., 358, 43–48, doi:10.1016/j.ijms.2013.11.006, 2014.

Zavala, M., Herndon, S. C., Slott, R. S., Dunlea, E. J., Marr, L. C., Shorter, J. H., Zahniser, M., Knighton, W. B., Rogers, T. M., Kolb, C. E., Molina, L. T., and Molina, M. J.: Characterization of on-road vehicle emissions in the Mexico City Metropolitan Area using a mobile laboratory in chase and fleet average measurement modes during the MCMA-2003 field campaign, Atmos. Chem. Phys., 6, 5129–5142, doi:10.5194/acp-6-5129-2006, 2006.
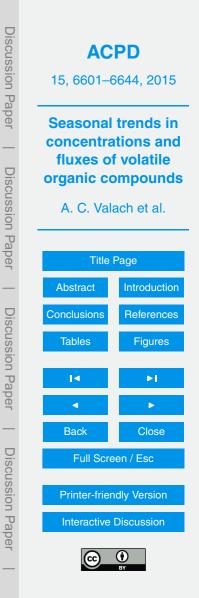
Table 1. Summary of instrument operating parameters and average meteorological conditions during the measurements in central London, August–December 2012.

Parameter	Unit	Mean (range)
Normalized sensitivity (S_N)[a]	$ncps\,ppb^{-1}$	11.5 (m/z 33), 13.3 (m/z 45), 10 (m/z 59), 4 (m/z 69), 3.6 (m/z 79), 2.5 (m/z 93), 1.5 (m/z 107)
Primary ion (m/z 19)	Cps	8.31×10^6 (6.14×10^6–1.15×10^7)
Water cluster (m/z 37)	Cps	1.92×10^5 (9.15×10^4–3.86×10^5)
	% of m/z 19	2.3 (1.5–3.4)
O_2^+	% of m/z 19	< 1.45 (1.11–2.01)
Temperature[b]	˚C	14.0 (−1.81–30.39)
Relative humidity	%	76 (50–97)
Pressure	mbar	1004.27 (968.71–1023.27)
Wind speed[b]	$m\,s^{-1}$	3.35 (0.12–14.96)
Friction velocity (u_*)[b]	$m\,s^{-1}$	0.5 (0.01–1.50)
SD of vertical wind speed (σ_w)[b]	$m\,s^{-1}$	0.65 (0.15–1.62)

[a] S_N: Normalized sensitivity as calculated using Taipale et al. (2008).
[b] Derived from measurements from the CSAT3 sonic anemometer (Campbell Scientific).

Table 2. Summary of 25 min VOC fluxes and mixing ratios above central London during August–Decebmer 2012.

Compound (m/z)	Methanol (m/z 33)	Acetaldehyde (m/z 45)	Acetone (m/z 59)	Isoprene (m/z 69)	Benzene (m/z 79)	Toluene (m/z 93)	C_2-benzenes (m/z 107)
Fluxes (mg m^{-2} h^{-1})							
Lifetime (OH[a])	12 d	8.8 h	53 d	1.4 h	9.4 d	1.9 d	5.9 h
N	2920	2811	2945	2119	1908	2315	2053
Min.	−2.91	−0.28	−1.74	−0.35	−0.64	−2.31	−3.27
1. quartile	0.12	0.06	0.10	0.02	0.002	0.08	0.04
Median	0.27	0.14	0.22	0.09	0.07	0.30	0.33
Mean	0.29	0.16	0.31	0.13	0.09	0.41	0.54
3. quartile	0.42	0.23	0.40	0.20	0.18	0.64	0.91
Max.	3.36	1.09	6.70	1.16	0.59	4.86	8.63
SD	0.25	0.15	0.37	0.16	0.15	0.53	0.86
Skew	0.86	1.27	4.39	1.18	0.32	1.75	2.33
Kurtosis	20.37	2.85	50.9	2.81	0.76	8.04	14.48
Mixing ratios (ppb)							
N	4834	4834	4834	4834	4834	4834	4834
Min.	5.73	< LoD (0.14)	< LoD (0.02)	< LoD (0.03)	< LoD (0.04)	< LoD (0.05)	< LoD (0.14)
1. quartile	6.82	0.59	< LoD (0.65)	< LoD (0.16)	< LoD (0.18)	< LoD (0.38)	< LoD (0.57)
Median	7.27	0.82	0.95	< LoD (0.22)	< LoD (0.24)	< LoD (0.54)	0.75
Mean	7.53	0.94	1.10	0.25	0.29	< LoD (0.65)	0.87
3. quartile	7.90	1.13	1.36	0.30	0.34	0.77	1.03
Max.	17.06	5.17	13.04	1.86	1.71	5.30	4.96
SD	1.12	0.53	0.68	0.14	0.19	0.45	0.50
Skew	2.21	2.14	2.60	1.97	2.80	3.07	2.79
Kurtosis	7.22	7.83	22.64	7.27	12.37	15.89	12.99
LoD[b]	0.96	0.45	0.66	0.25	0.28	0.66	0.71

[a] Atmospheric lifetimes with regard to OH for a 12 h daytime average OH concentration of 2.0×10^6 molecules cm^{-3} (Atkinson, 2000).

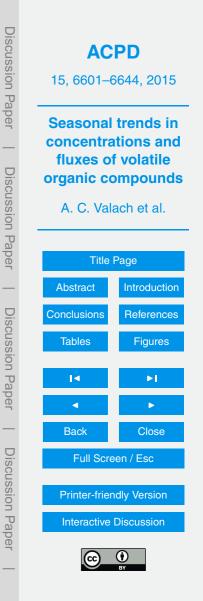[b] LoD: Limit of detection calculated using Taipale et al. (2008).

Table 3. Summary of site meteorology by month in central London during 2012.
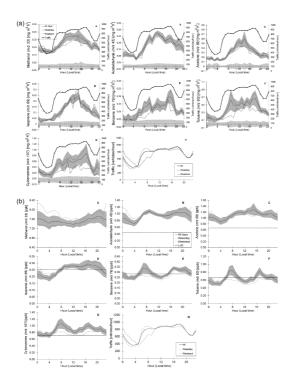
Parameter	Data coverage (%)	Median stability (ζ)	Wind speed ($m\,s^{-1}$)	Dominant wind direction (%)	Footprint[*] length (m)	Footprint width (m)
Aug	67	−0.0086	3.3	S (54)	2417	1355
Sep	83	−0.0154	3.2	W (48)	1285	880
Oct	89	−0.0006	3.5	S (29)	2624	1327
Nov	51	−0.0037	3.4	S (53)	2329	1156
Dec	40	0.0047	3.4	N (32)	1804	990

[*] Calculated two-dimensional description of the oval footprint according to the KM model. Length parameter is the length between the point nearest to the sensor where the crosswind-integrated footprint function reaches 1 % of its maximum value to the point where it drops below 1 % of the maximum value.

Figure 1. Map of central London overlaid with the Ordinance Survey grid including the measurement location at King's College (green point) with references to the geography of Greater London and Great Britain.
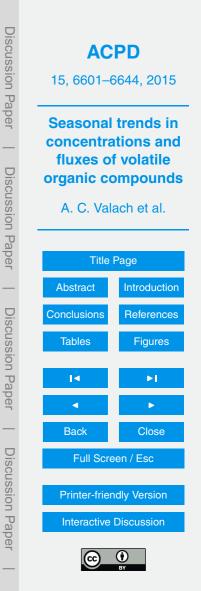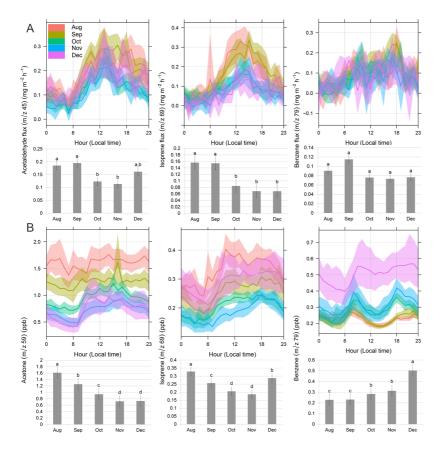
Figure 2. (a) Average diurnal profiles in local time for selected VOC fluxes ($mg\,m^{-2}\,h^{-1}$) separated into all days, weekdays and weekends with traffic (vehicles h^{-1}), detection limit (patterned area), and upper and lower confidence intervals (shaded area). Compounds are: m/z 33 (methanol), m/z 45 (acetaldehyde), m/z 59 (acetone/propanal), m/z 69 (isoprene/furan), m/z 79 (benzene), m/z 93 (toluene), and m/z 107 (C_2-benzenes). **(b)** Average diurnal profiles in local time for selected VOC mixing ratios (ppb) separated into all days, weekdays and weekends with detection limit (dotted line), and upper and lower confidence intervals (shaded area). Compounds are: m/z 33 (methanol), m/z 45 (acetaldehyde), m/z 59 (acetone/propanal), m/z 69 (isoprene/furan), m/z 79 (benzene), m/z 93 (toluene), and m/z 107 (C_2-benzenes).
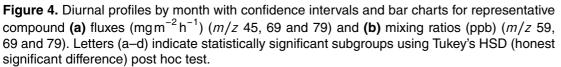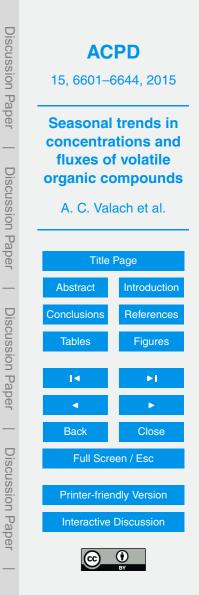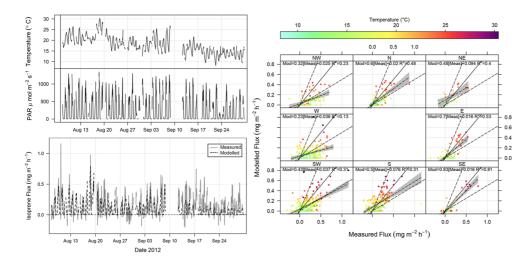
Figure 3. Examples, using isoprene, of averaged VOC fluxes (left) and mixing ratios (right) as a function of photosynthetically active radiation (PAR) ($\mu mol\, m^{-2}\, s^{-1}$), temperature (°C) and traffic density (vehicles h^{-1}) based on 25 min VOC means with linear or exponential regressions, formulae, R^2-values and detection limit (shaded area for fluxes and dashed line for mixing ratios).
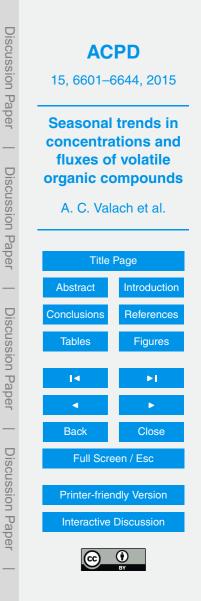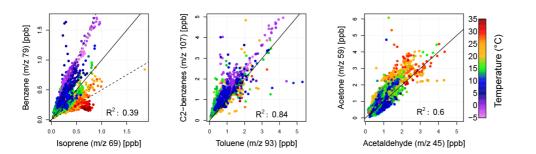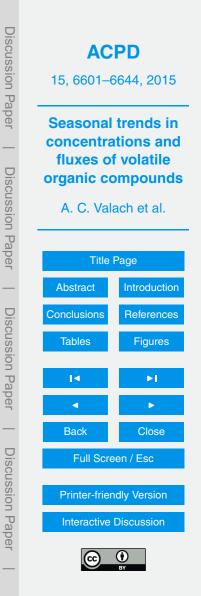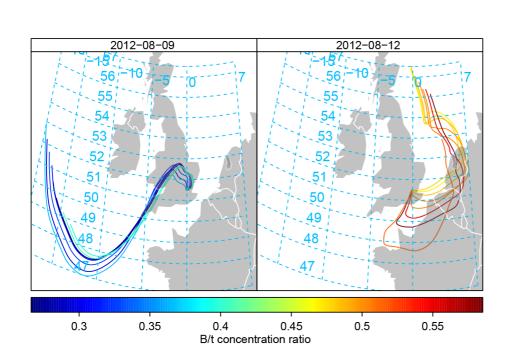
Figure 4. Diurnal profiles by month with confidence intervals and bar charts for representative compound **(a)** fluxes (mg m^{-2} h^{-1}) (m/z 45, 69 and 79) and **(b)** mixing ratios (ppb) (m/z 59, 69 and 79). Letters (a–d) indicate statistically significant subgroups using Tukey's HSD (honest significant difference) post hoc test.

Title Page

Abstract | Introduction

Conclusions | References

Tables | Figures

◄ | ►

◄ | ►

Back | Close

Full Screen / Esc

Printer-friendly Version

Interactive Discussion

Figure 5. Right: correlation between modelled and measured isoprene fluxes ($\mathrm{mg\,m^{-2}\,h^{-1}}$) by wind direction using the G95 algorithm with temperature as a third variable, OLS regression lines, 99th confidence intervals, formulae, and R^2-value. Left: time series of both measured (grey) and modelled (black) fluxes, as well as PAR and temperature measurements for August and September 2012.
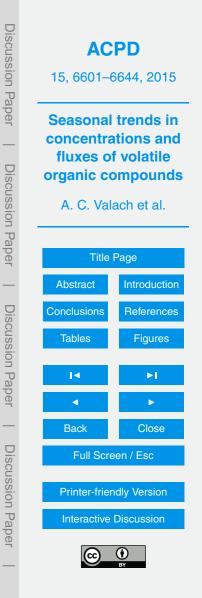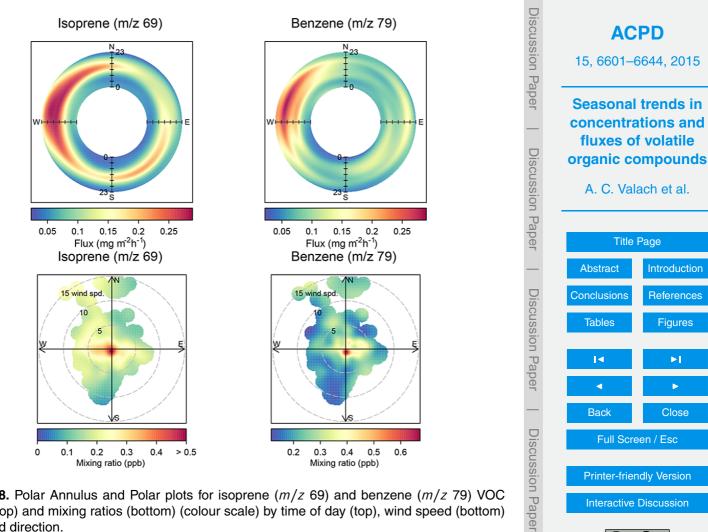
Figure 6. Selected scatter plots of representative VOC/VOC mixing ratio correlations with temperature as a third variable showing an example of bimodal, strong linear and medium linear correlations with R^2-values, 1 : 1 line, 1 : 2 and 2 : 1 lines for the bimodal example in the left panel.

Figure 7. 24 h back trajectories from the NOAA HYSPLIT trajectory model during selected days in August 2012 corresponding to periods of low (left) and high (right) benzene/toluene concentration ratios. Daily release in 3 h intervals (10 m height) for 24 h prior.
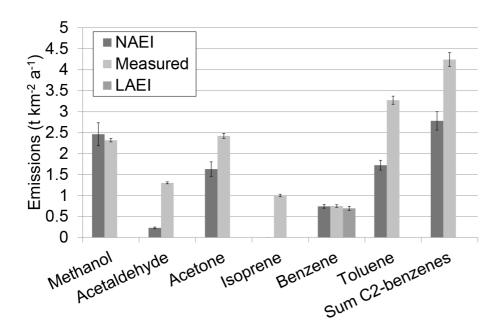
Figure 8. Polar Annulus and Polar plots for isoprene (m/z 69) and benzene (m/z 79) VOC fluxes (top) and mixing ratios (bottom) (colour scale) by time of day (top), wind speed (bottom) and wind direction.

Title Page

Abstract | Introduction

Conclusions | References

Tables | Figures

|◄ | ►|

◄ | ►

Back | Close

Full Screen / Esc

Printer-friendly Version

Interactive Discussion

Figure 9. Bar chart showing up-scaled comparisons of LAEI and NAEI estimates against measured fluxes in $t\,km^{-2}\,a^{-1}$ for speciated VOCs with error bars.